Available online at www.sciencedirect.com
ScienceDirect
Polymer 48 (2007) 1287–1296
polymer
www.elsevier.com/locate/polymer

Characterisation of the supramolecular structure of chemically and physically modified regenerated cellulosic fibres by means of high-resolution Carbon-13 solid-state NMR

Roger N. Ibbett [a,*], Dimitra Domvoglou [a], Mario Fasching [b]

[a] *Christian Doppler Laboratory for Textile and Fibre Chemistry in Cellulosics, School of Materials, University of Manchester, Manchester M60 1QD, UK*
[b] *K+, Kompetenzzentrum Holz GmbH, Saint-Peter-Street 25, 4021 Linz, Austria*

Received 3 August 2006; received in revised form 8 December 2006; accepted 17 December 2006
Available online 20 December 2006

Abstract

Carbon-13 high-resolution solid-state NMR techniques have been invaluable in elucidating the structure of regenerated cellulosic materials. Studies of a range of fibres have shown systematic changes in chemical shifts, which can be related to the influences of physical processing or chemical modification. A constrained curve fitting method has been applied, where the C4 spectral envelope is represented as the sum of contributions from polymer in ordered, partially-ordered and disordered environments, associated with differing conformational arrangements of the cellulose hydroxymethyl and glycocidic bonds. The empirical gamma-*gauche* effect seems likely to provide the best rationalization for the relationship between C4 shifts and conformational order, taking into account the increased range of bond angles in disordered environments. The quantification of proportions of polymer units within different conformational groupings will provide new insights into the development of supramolecular texture. This will allow better appreciation of the relationships between fibre processing and ultimate fibre performance.

Keywords: Cellulose; NMR; Structure

1. Introduction

Cellulose is processed on a large industrial scale in the manufacture of fibres, films and other structural products. This often involves solubilisation or chemical derivatisation, which may cause the complete disruption of the native semi-crystalline morphology and the recombination of polymer chains into a new regenerated morphology. Dissolution and regeneration typically result in the formation of crystals of the cellulose II allomorph, as opposed to the original native cellulose I form. In addition, the supramolecular structure maybe entirely different from that of the raw material, potentially with crystalline domains interspersed within regions of disorder. Disorder may also exist as crystalline defects or imperfections at crystallite surfaces, with the details of the morphology depending to a great extent on processing conditions. In turn, the adjustment of processing environment will have an impact on the resulting properties and performance of the formed material, especially on its mechanical properties and response to moisture. The study of supramolecular structure is therefore of great commercial interest, having a direct bearing on the development of new regenerated products and the control of consistency and quality of existing products, including fibres, films, tapes, sponges and powders.

Carbon-13 high-resolution solid-state NMR techniques have been invaluable in elucidating the structure of cellulosic materials [1,2]. Considerable detail has been gathered concerning the various crystalline polymorphic forms present in both natural and regenerated products, based on the assignment of chemical shifts of different carbon sites [3,4]. The quantitative analysis of cellulose Carbon-13 spectra is used routinely for determining the fractional crystalline content of cellulosic

* Corresponding author. Tel.: +44 1613063173.
E-mail address: roger.ibbett@manchester.ac.uk (R.N. Ibbett).

0032-3861/$ - see front matter © 2007 Elsevier Ltd. All rights reserved.
doi:10.1016/j.polymer.2006.12.034

samples, complementing data from wide-angle X-ray diffraction techniques [5–7]. In addition, spectral editing on the basis of molecular dynamics has revealed much more detail about the semi-crystalline morphology of both natural and regenerated cellulose materials [8,9]. Such techniques have highlighted differences between surface and internal crystalline order [10].

Much of the detail in the chemical shift spectrum is associated with the cellulose C4 envelope, which is especially sensitive to the extent of stereochemical order and the range of conformational environments of the repeat unit [10,11]. Significant differences in C4 chemical shifts have been found for the non-crystalline regions of natural and regenerated sources of cellulose, believed to be related to the C4–C5–C6–O6 rotameric state [10]. This has been interpreted on the basis of the semi-empirical gamma-*gauche* or related effects, which also provide an explanation for the chemical shifts of other natural and synthetic polymers [12–14]. At present this seems the most hopeful approach for rationalizing the breadth of the C4 envelope, although other influences due to stereochemistry of hydrogen bonding should not be completely ruled out. A fuller appreciation of the origins of C4 chemical shifts will be of immense value in the characterization of regenerated cellulose phase structure, with the prospect of establishing more meaningful values for total crystallinity. In addition, the subdivision of the intensities within the C4 envelope may provide more quantitative information about types of disorder, allowing a more complete picture to be developed of the phase structure of regenerated cellulosic materials.

This study has concentrated on the investigation of the Carbon-13 spectral features of two contrasting regenerated cellulosic fibre types: low-crystallinity viscose fibre (from the xanthate process) and higher crystallinity lyocell fibre (from the *N*-methylmorpholine-*N*-oxide process). Fibre samples have been subjected to various chemical and physical post-treatments, with special attention given to the interpretation of the resulting changes to the C4 envelope. In addition, spectra have been obtained of a wider selection of regenerated cellulosic fibre types, including those from other manufacturing routes. This has allowed the mapping of chemical shift behaviour to be extended to cover the limits of morphologies achievable by commercial processing. Proton H-$T_{1\rho}$ relaxation time editing has been performed on selected samples and an examination has been carried out of the influence of hydration and dehydration treatments on spectral features and molecular dynamics.

2. Experimental

Samples of lyocell and viscose fibres were provided by Lenzing AG. These were 1.3 dtex staple products, both from regular commercial supplies. An extended set of cellulosic fibre types was also made available, also courtesy of Lenzing AG. These were, fortisan (high modulus fibre made via saponification of cellulose acetate), cupro (fibrillar fibre made via cuprammonium hydroxide complex solution method), modal (high wet modulus fibre made via xanthate route), polynosic (fibrillar, high orientation fibre made via xanthate route), and tire cord (high modulus, high strength fibre made via xanthate route).

NMR measurements were carried out using a Bruker AVANCE instrument at 75 MHz carbon frequency. A Bruker double-air-bearing Magic Angle Spinning (MAS) probe was employed for all work, operating with 7 mm external diameter sample rotors, with sample spinning at 4 kHz. A ramped contact-power cross-polarisation (CP) pulse sequence was applied [15], with a total of 1 ms contact time. A proton B1 field of approximately 45 kHz was set for both the CP step and high-power proton decoupling, with a 3 s T_1 relaxation delay between each pulse cycle. A delayed contact CP sequence was also employed for measurement of selected samples [16], to examine the relaxation of magnetization in the B1 field. Proton rotating frame relaxation time constants (H-$T_{1\rho}$) were determined by exponential fitting of the C4 peak intensities, delineated between fixed chemical shifts, against the incremented contact time delay. Data from approximately 1000 pulse cycles were accumulated for each CPMAS measurement and 600 cycles for each delayed contact increment. All spectra were processed with 20 Hz exponential line-broadening. Chemical shift referencing was performed using an external adamantane standard, with the CH (high-field) peak set at 29.50 ppm.

Lyocell and viscose fibres were examined in the as-received dry-state, then in the wetted state with 20–35% added water, and then re-dried at ambient temperature back to levels of natural moisture content (at approximately 40% RH). Samples from the wider group of cellulosic fibres were measured in the dry-state without additional preparation.

A portion of the lyocell fibre was subjected to high-energy mechanical degradation using a metal ball-mill. CPMAS spectra were acquired after 20 and 60 min milling times, although measurements after longer times were not possible due to metallic contamination and the detrimental effect on spectral resolution. A further lyocell sample was treated with sodium monochloroacetate (SMCA) under strong alkaline swelling conditions. The treatment solution was made up with 10% by weight NaOH and 20% SMCA in water, held at room temperature. A portion of fibre was immersed in the solution for 2 min, which was then squeezed between two pad-rollers to a liquor content of approximately 120% of initial fibre weight. The padded sample was incubated in a sealed polyethylene bag at 70 °C for 20 min, and was then rinsed thoroughly in a 50/50 mixture of isopropyl alcohol (IPA) and water. Final rinsing was carried out using 100% IPA which was allowed to evaporate under ambient conditions overnight. CPMAS and delayed contact measurements were performed on the carboxymethylated product (CM-lyocell). From the CPMAS spectrum it was possible to determine the peak area of the carboxymethyl carbonyl group. An overall detection efficiency of this peak of 65% compared to the cellulose C1 integral was assumed [17], from which it was possible to confirm the degree of substitution (DS) of the derivatised product.

Further samples of viscose and lyocell were subjected to acid hydrolysis. Portions of fibre were immersed in excess

1 M sulphuric acid and then incubated in covered beakers in a water bath at 95 °C for 5 h. The powdered microcrystalline products (MC-lyocell and MC-viscose) were filtered, washed and then neutralized in a pH buffer before final rinsing in distilled water followed by drying in a laboratory oven at 80 °C.

3. Results

The full-scale Carbon-13 CPMAS spectra of viscose and lyocell are shown in Fig. 1. The C4 region between 91 and 82 ppm provides most detail concerning the material phase texture, comprising a series of overlapped peaks, as illustrated in Fig. 2. The assignment of shifts associated with C4 crystalline sites is well documented, with the two convoluted peaks referenced at 89.4 and 88.3 ppm believed to be due to two non-equivalent crystallographic positions within the cellulose II unit cell [18]. The intensity to higher field is from cellulose molecular conformations where full crystalline uniformity has been lost [19,20]. This non-crystalline feature extends from approximately 90 to below 80 ppm, overlapping the crystal peaks and the larger neighbouring C2,3,5 envelope. As can be seen in Fig. 2, the appearance of the non-crystalline intensity is dependent on material processing, with ball-milling increasing the contribution of this feature in the spectrum of lyocell, and shifting the apparent maximum from 85.3 to 84.2 ppm. The sensitivity of the non-crystalline feature with respect to sample history is also clear in Fig. 3, where the C4 regions for the series of cellulosic fibre types are overlaid, with intensities normalized to the 89.5 ppm crystalline peak. Superficially, the non-crystalline feature shifts to higher field as its relative intensity grows, suggesting a relationship between the amount and the averaged environment of the disordered polymer, which in turn depends on the source of the regenerated fibre [10]. Fig. 1 also shows that the relative intensity of the non-crystalline feature is higher in viscose than in lyocell, and at lower chemical shift in viscose. The trends for all samples are summarised in Table 1.

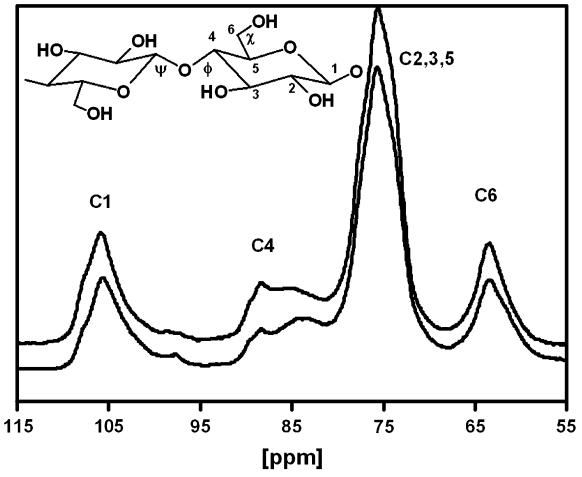

Fig. 1. Full-scale Carbon-13 CPMAS spectra of regenerated cellulosic fibres: upper = lyocell, lower = viscose.

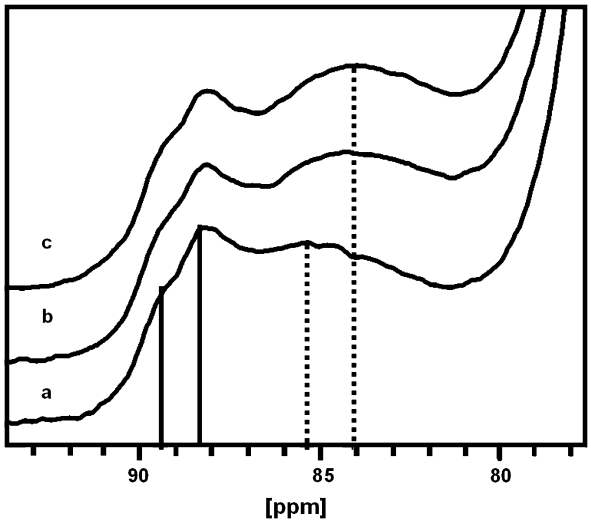

Fig. 2. Expansion of C4 region of Carbon-13 CPMAS spectrum of lyocell fibre: (a) dry as-received, (b) ball-milled for 20 min, (c) ball-milled for 60 min.

The preparation of the CM-lyocell product was via the swollen alkali-cellulose intermediate, where the pH was sufficiently high for all cellulose hydroxyl groups to be fully deprotonated. In this state the sodium counterions are believed to permeate the entire structure, with the $1\bar{1}0$ planes separated at a greater distance than in the cellulose II crystalline solid [21]. The SMCA reagent was therefore assumed to be fully accessible to both crystalline and non-crystalline regions, allowing reaction on a statistical basis along each polymer chain. The target DS of 0.15–0.2 was designed to introduce sufficient numbers of functional groups to inhibit the reformation of cellulose II crystals after washing and drying, but without introducing a significant proportion of new chemical shifts from derivatised 2, 3, or 6 carbons. The CM-lyocell spectrum should therefore represent that of a physically modified material with little or no crystallinity and with no fixed

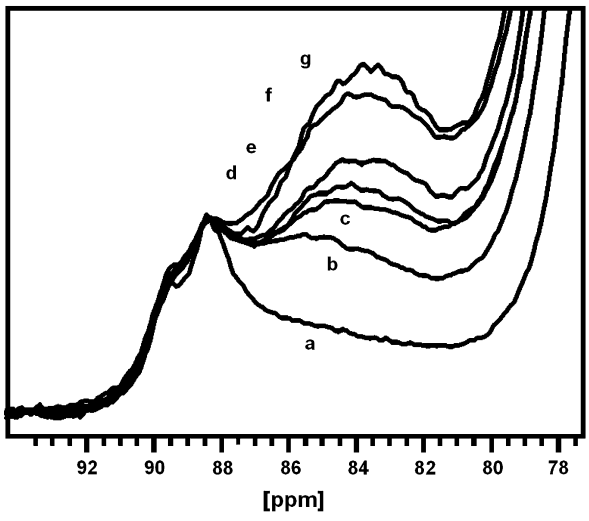

Fig. 3. Expansion of C4 region of Carbon-13 CPMAS spectra of a series of regenerated cellulosic fibres: a = tire cord, b = polynosic, c = viscose, d = modal, e = cupro, f = lyocell, g = fortisan.

Table 1
Experimental and fitted features of the CPMAS Carbon-13 C4 spectral region of regenerated cellulosic fibre materials

Fibre sample	Non-crystalline feature apparent shift maximum (ppm)	Fitted crystalline-ordered intensity (%); $\delta = 89.5 + 88.3$ ppm, FWHH = 125 Hz	Fitted partially-ordered intensity (%); $\delta = 86.8$ ppm, FWHH = 315 Hz	Fitted fully-disordered intensity (%); $\delta = 83.2$ ppm, FWHH = 490 Hz[a]	Partially-ordered to crystalline-ordered intensity ratio
Fortisan	85.5	32.9	25.2	41.9	0.77
Lyocell	85.3	16.7	26.1	57.1	1.56
Cupro	84.6	13.8	18.0	68.2	1.30
Modal	84.3	13.4	16.1	70.5	1.21
Viscose	83.8	13.3	12.9	73.7	0.97
Polynosic	83.8	8.9	12.2	78.8	1.37
Tire cord	83.6	8.7	8.1	83.2	0.93
Ball-milled lyocell (20 min)	84.5	15.2	18.0	66.8	1.18
Ball-milled lyocell (60 min)	84.2	14.4	16.9	68.7	1.17
Carboxymethylated lyocell	84.0	2.7	8.8	88.4 (83.5 ppm)	3.26
Wetted and re-dried lyocell	85.3	20.2	27.9	51.9	1.38
Wetted and re-dried viscose	83.5	12.7	13.7	73.6	1.08
Microcrystalline lyocell	85.5	42.0	31.4	26.6	0.75
Microcrystalline viscose	85.0	36.9	22.3	40.8	0.60

[a] Neighbouring C2,3,5 peak parameters are: $\delta = 75.5$ ppm, FWHH = 375 Hz.

conformations of the C4–O1–C1 glycocidic linkages (ϕ and ψ angles by convention). The expansion of the C4 region of the CM-lyocell product is shown in Fig. 4, superimposed over the same spectral region of the original fibre. This confirms the almost total absence of crystalline peaks and the dominance of a broad peak centred around 84 ppm, which according to the conformational definition is now assigned to fully-disordered polymer. This broad peak is very similar to that which becomes dominant at lowest crystalline intensities in the fibre series in Fig. 3, seen at a slightly lower chemical shift at 83.6 ppm.

Acid hydrolysis is known to occur preferentially in the non-crystalline accessible polymer regions in cellulosic materials, randomly breaking glycocidic linkages and allowing the dissolution of low molecular weight fragments [22]. This is accompanied by the recrystallisation of material at crystallite surfaces, causing an apparent increase in crystal size and perfection [23]. A comparison of the C4 region before and after hydrolysis is shown for lyocell in Fig. 5, and for viscose in Fig. 6, with spectra obtained using standard CPMAS acquisition conditions. After hydrolysis the crystalline peaks of both fibres, at 89.4 and 88.3 ppm, become slightly more resolved with increased intensity. This is accompanied by a significant reduction in intensity of the C4 non-crystalline features to higher field, at around 84 ppm. The changes are consistent with the expected conversion brought about by hydrolysis, with a high proportion of the accessible polymer either solubilised or recrystallised as a result of reaction in the acid solution. Residual intensity at non-crystalline shift positions is therefore probably associated with polymer sites that are either

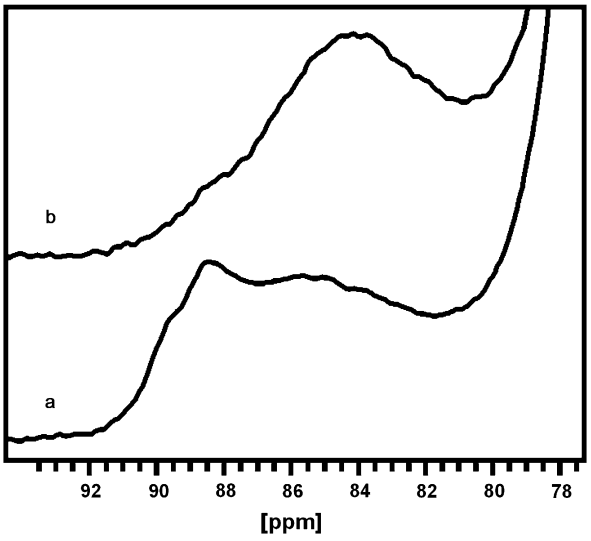

Fig. 4. Expansion of C4 region of Carbon-13 CPMAS spectrum of: (a) original lyocell fibre and (b) carboxymethylated lyocell fibre with DS of approximately 0.2 (CM-lyocell).

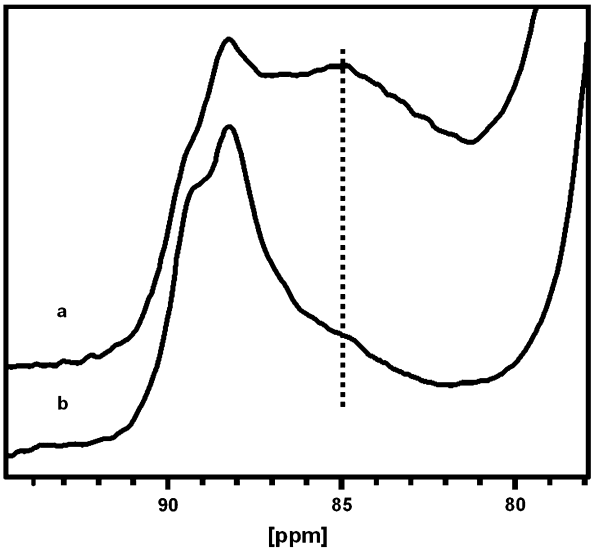

Fig. 5. Expansion of C4 region of Carbon-13 CPMAS spectrum of: (a) original lyocell fibre and (b) lyocell fibre hydrolysed with 1 M sulphuric acid for 5 h at 95 °C (MC-lyocell).

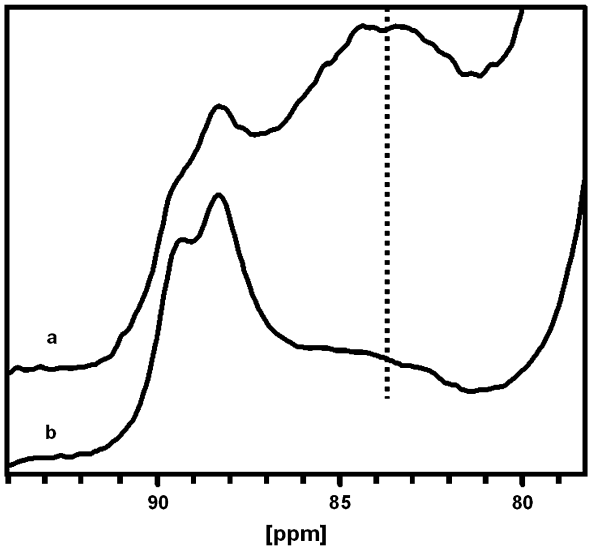

Fig. 6. Expansion of C4 region of Carbon-13 CPMAS spectrum of: (a) original viscose fibre and (b) viscose fibre hydrolysed with 1 M sulphuric acid for 5 h at 95 °C (MC-viscose).

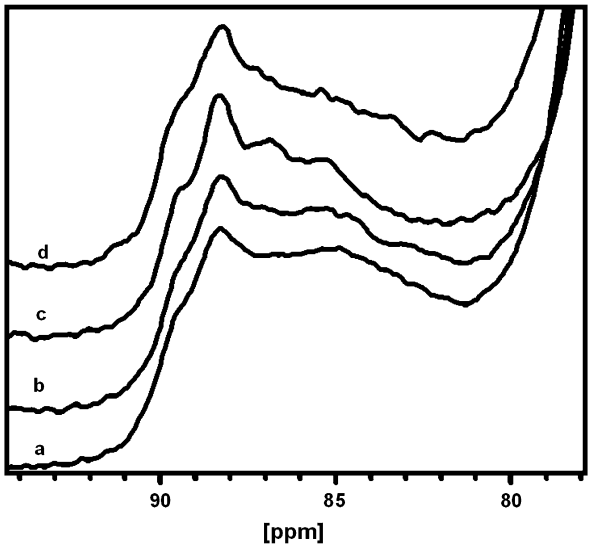

Fig. 7. The effect of wetting and re-drying on the Carbon-13 C4 shifts of lyocell fibre, via CPMAS acquisition: (a) initial dried fibre, (b) fibre with 20% added water by weight, (c) fibre with 30% added water, (d) fibre re-dried at ambient temperature.

unreactive or inaccessible towards the acid, most likely at crystal interfaces or internal crystal defects [22]. Fig. 5 shows that the intensity of the residual feature in the MC-lyocell spectrum is weighted at around 85 ppm, which is higher than the shifts identified with environments having full conformational disorder. This distinct chemical shift region has therefore been assigned to polymer environments with partial conformational order, with the cellulose glycocidic linkages maintaining the same conformations as the crystal environments, but with the C5–C6 bond exhibiting rotameric freedom [9]. The shoulder at 85 ppm in the MC-lyocell spectrum matches the position of the larger non-crystalline feature in the initial lyocell spectrum, suggesting that the original lyocell fibre may have population of polymer sites of partial order, and therefore possibly a high proportion of crystal interfaces. The spectrum of MC-viscose, in Fig. 6, also shows residual non-crystalline intensity at a position above 84 ppm, again probably due to crystal defects or interfaces. Here, there is a difference in shift compared to the non-crystalline feature in the original fibre at 83.6 ppm, suggesting that the initial viscose fibre, in contrast to lyocell, contains a lower proportion of partially-ordered polymer within interfacial environments.

Wetting treatments are known to modify the Carbon-13 spectral features of cellulosic materials [24], as water induced plasticization causes a readjustment of polymer bond conformations. Water is not believed to access crystalline interiors so the shifts for cellulose II at 89.5 and 88.3 ppm are not expected to change. Fig. 7 shows the action of wetting on lyocell, where only the non-crystalline C4 shifts are affected, as the amount of added water exceeds 30% of total weight. This level of saturation is presumably required to induce effective conformational freedom of the C5–C6 bond and also the C4–O1–C1 bonds, which may be possible at the accessible crystal–water interfaces. The non-crystalline peak appears to resolve into two sharper features, at 87 and 85.2 ppm, as observed for other regenerated cellulosic fibres [11,24]. For lyocell the spectrum of the wetted fibre also reveals a sharpening of the crystalline features, which maybe a manifestation of plasticization induced crystallisation. Disordered interfacial and defect sites apparently gain sufficient backbone conformational freedom for crystals to achieve more extended perfection. The spectrum of re-dried lyocell fibre shows that after removal of water the intensity is retained at the crystalline shift positions at 89.5 and 88.3 ppm, which appears to be at the expense of intensity below 85 ppm. The high proportion of interfacial disordered polymer environments makes lyocell especially sensitive to recrystallisation under these wet treatment conditions, which is apparently not reversible.

Some evidence of wetting induced plasticization is also seen for viscose fibre. A slight shift of intensity from non-crystalline to crystalline positions is apparent, in Fig. 8, although this is not as dramatic as seen with lyocell. Viscose contains higher amount of disordered material than lyocell, as evidenced by the shift at 83.6 ppm, which may not be associated with crystal interfaces. Recrystallisation is therefore not as efficient. In addition, re-drying appears to reverse the intensity changes, suggesting that the removal of water allows bond conformations to freeze again into a more randomized distribution.

Changes in spectral intensities on wetting could also be due to the effect of molecular dynamics on the CPMAS experiment. Proton H-$T_{1\rho}$ relaxation times can provide information about local molecular dynamics and also sample spatial heterogeneity through the influence of proton spin-diffusion. The CPMAS intensities of the main carbon chemical shifts were each fitted to a single exponential function, with data recorded for wet and dry viscose and lyocell fibres, dry ball-milled lyocell and CM-lyocell, as summarised in Table 2. Integration of the C4 crystalline intensity was from 90 to 87 ppm and the C4 non-crystalline intensity from 86 to 82 ppm. For each sample the H-$T_{1\rho}$ time constants at all carbon sites are

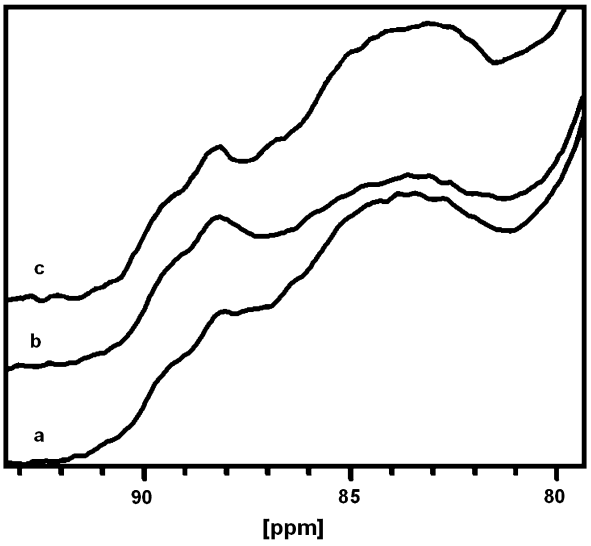

Fig. 8. The effect of wetting and re-drying on the Carbon-13 C4 shifts of viscose fibre, via CPMAS acquisition: (a) initial dried fibre, (b) fibre with 30% added water by weight, (c) fibre re-dried at ambient temperature.

similar, indicating the presence of spin-diffusion averaging. However, differences between relaxation times for C4 crystalline and non-crystalline shifts are observed for all samples, which suggest the existence of separate morphological domains [1]. Multi-exponential behaviour might therefore be expected at the other carbon sites, where shifts from crystalline and non-crystalline domains are superimposed, although this cannot be resolved with the limited numbers of time increments used for these experiments. Diffusional averaging is complete over distances less than 2–3 nm so the partial averaging of C4 relaxation is consistent with the existence of crystalline domains slightly larger than this scale [25]. The CM-lyocell sample, which has almost full conformational disorder, exhibits H-$T_{1\rho}$ relaxation times of only 3 ms compared to 7 ms for the original fibre. This lower value may represent the intrinsic character of a fully-disordered phase within a semi-crystalline two-phase texture, in the absence of spin-diffusion averaging. However, the steric disruption caused by the carboxylate groups could possibly lead to an enhanced plasticising action, lowering the H-$T_{1\rho}$ relaxation times further than experienced by a non-derivatised polymer.

From Table 2, it is seen that viscose has slightly lower H-$T_{1\rho}$ relaxation times than lyocell, which is consistent with the lower crystalline content of the fibre. If the intrinsic crystalline and non-crystalline relaxation times are assumed to be constant, then from simple statistics the existence of spin-diffusion would lead to a lower weighted values measured at both shift positions. The action of ball-milling also appears to cause a reduction of H-$T_{1\rho}$ relaxation times for lyocell, which is consistent with the observed reduction in crystalline content due to mechanical action, again leading to a lowering of the population weighted averages.

The action of wetting brings about a small but consistent lengthening of all proton H-$T_{1\rho}$ relaxation times, shown in Table 2, for both crystalline and non-crystalline C4 shift positions. This is seen for both viscose and lyocell, from the lyocell data the increase appears to correlate with the amount of added water. The action of water is not believed to seriously disturb the efficiency of the CPMAS experiment, with previous studies of Carbon-13 T_1 relaxation suggesting that the polymer carbons and directly attached protons still have solid-like properties, as required for polarisation transfer [8]. Relaxation of magnetization in the rotating frame requires motional processes at the B1 frequency, with softening by plasticization or decrystallisation increasing relaxation efficiency and reducing H-$T_{1\rho}$ times. This is the effect seen after ball-milling or chemical derivatisation. Conversely, the rising H-$T_{1\rho}$ times suggests a reduction in relaxation efficiency, which maybe due to the motional decoupling of cellulose hydroxyl groups by fast exchange with added water. This would therefore reduce the total number of protons available as a relaxation sink.

Additional delayed contact CPMAS measurements were carried out on wetted viscose using either a 0 or 8 ms H-$T_{1\rho}$ relaxation delay, for spectral editing purposes. Slower relaxing polymer material is relatively enhanced at longer delay times, which is displayed in the absence of faster relaxing polymer after subtraction, as shown in Fig. 9. Crystalline peaks are seen at 89.5 and 88.3 ppm in the difference spectrum of viscose, with disordered intensity at 84 ppm almost absent. Residual intensity in the difference spectrum at around 85–87 ppm is consistent with the shift position of polymer sites with partial conformational order, assigned in the spectra of the hydrolysed samples. These environments must have rigid character, which supports the interpretation that they are associated with crystal defects or interfaces, but do not have full crystalline registration. Viscose is expected to have a low intensity from partially-ordered polymer, given the low overall crystallinity of this fibre. The proportion of partially-ordered intensity relative to crystalline intensity may provide information concerning crystal size and perfection, as will be discussed.

Table 2
Proton rotating frame relaxation times for main Carbon-13 peaks of different cellulosic fibre materials

Sample	H-$T_{1\rho}$ (ms)				
	C1	C4 (90–87 ppm)	C4 (86–82 ppm)	C2,3,5	C6 (90–87 ppm)
As-received viscose	6.1	6.7	5.6	5.9	6.0
Viscose + 30% water	8.1	9.1	7.2	7.8	7.8
As-received lyocell	7.3	8.1	6.3	6.8	6.8
Lyocell + 20% water	9.5	10.4	8.4	8.9	8.8
Lyocell + 30% water	11.2	12.1	9.8	10.9	10.1
Lyocell after 60 min ball-milling	6.5	7.1	5.7	6.2	6.3
Carboxymethylated lyocell	3.1	–	2.9	3.1	3.1

4. Discussion

The range of chemical shifts associated with the C4 region of regenerated cellulosic materials suggests a quite

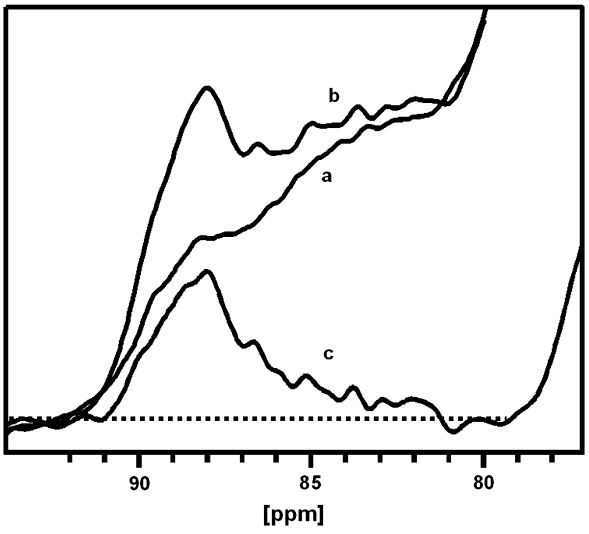

Fig. 9. C4 region of Carbon-13 CPMAS spectra of viscose fibre with: (a) no H-$T_{1\rho}$ relaxation delay, (b) 8 ms delay, (c) difference showing components with longer relaxation times from more rigid material.

complicated phase texture, consisting of polymer in a spread of conformational environments. Some of these environments have been assigned with a high degree of confidence, particularly those relating to full crystalline order. Both acid hydrolysis and H-$T_{1\rho}$ editing techniques lead to enhanced intensity at recognized peak positions [9,18] with shifts referenced in this work at 89.5 and 88.3 ppm, as illustrated for lyocell in Fig. 2.

The assignment of C4 features due to conformationally disordered polymer can also be performed with some confidence. The effect of ball-milling, or chemical randomisation, or variation in fibre manufacturing all lead to the enhancement of a broad peak centred at around 83–84 ppm, as illustrated in Fig. 3. This polymer material represents a state where a range of conformations are present, rather than the fixed conformations demanded by crystalline order. The hydroxymethyl C5–C6 bonds (χ angle) and the glycocidic C1–O1–C4 bonds (ϕ and ψ angles) are all expected to be variable.

Intensity at intermediate C4 shift positions represents polymer with partial conformational order (or disorder). From the spectra of the hydrolysed fibres it is reasonable to assign a large proportion of residual non-crystalline intensity to material at crystal interfaces, as in Fig. 5, where the pendant cellulose hydroxymethyl group has additional freedom. Such characteristic C4 shifts are therefore probably a result of variations of only the C5–C6 bond conformations with the C1–O1–C4 bonds retaining crystalline conformational positions [10,26,27]. This interfacial contribution is prevalent in lyocell, reflecting the fibrillar character of the fibre [28,29]. Wetting disturbs the solid hydrogen-bonding network of cellulose, leading to improved conformational freedom within the accessible regions of the structure. This is also noticed particularly with lyocell, where further recrystallisation is permanent following drying. The new resolved shifts in wetted lyocell are likely to be caused by a redistribution of C5–C6 bond angles towards more favourable energies. However, plasticization is likely to allow exchange between more than one rotameric minimum, leading to an environment described by an weighted average [24].

An appreciation of the proportions of polymer chains with different conformational states would allow changes in supramolecular structure to be followed due to fibre processing or manufacturing history. Such analysis may be achieved by careful spectral simulation, provided that constraints applied to the fitting exercise are consistent with the underlying polymer organisation. A curve fitting exercise has therefore been carried out using the Solver non-linear error minimization tool (Excel, Microsoft Inc.), in an attempt to describe the full C4 spectral envelope as a combination of intensities from four separate peaks, representing different degrees of conformational order. This should provide the simplest and most robust simulation solution, underpinned by the qualitative assignments discussed. Two sharp peaks of equal intensities with established shifts at 89.5 and 88.3 ppm have been selected to account for crystalline (ordered) polymer, with fixed ϕ, ψ and χ angles. A third broader peak with a shift at 86.8 ppm has been selected to account for polymer at interfaces and defects (partially-ordered), where the glycocidic ϕ, ψ angles are fixed at the crystalline positions but the C5–C6 χ angle is variable. The additional width of this peak is designed to account for the statistical spread of conformational positions associated with the C5–C6 bond. The shift maximum for the peak is based partly on the position of the residual non-crystalline intensity in the H-$T_{1\rho}$ edited sub-spectrum, in Fig. 9, and also on the spectra of the microcrystalline products, in Figs. 5 and 6. Lastly, an even broader peak is selected at 83.2 ppm, to account for polymer (fully-disordered) where χ, ϕ and ψ angles are all variables. The increased width assumed for this peak follows the greater range of possible conformational arrangements and the increased statistical spread of chemical shifts. The value of the shift maximum is taken from extrapolation of the experimental disordered peak positions with reducing crystallinity for the fibre series, Fig. 3 and Table 1.

Gaussian shapes have been assumed throughout and the positions and widths for the fitted peaks have been fixed during the fitting exercise. Improved simulated spectra could no doubt be achieved by removal of constraints, but at the expense of the physical meaning attached to the peak assignments. The crystalline peaks may in reality have some Lorenzian character, which would resolve them better and account for additional wing intensity, however, this would add another unwanted variable parameter. Peak shape effects due to chemical shift anisotropy are considered negligible for all cellulose carbon sites with MAS spinning at 4 kHz [30], with no additional narrowing achieved by spinning at higher speeds. A single large peak was set at 75.5 ppm to account for the neighbouring C2,3,5 envelope, of adjustable height but fixed width and position, as summarised in Table 1.

Examples of the fitting exercise applied to viscose, lyocell, CM-lyocell and MC-lyocell are shown in Figs. 10–13. The fitted parameters for the individual fitted peaks are presented in Table 1. As is shown, the combination of different intensities of the separate partially-ordered and fully-disordered peaks leads to variations in the maximum position of the resulting

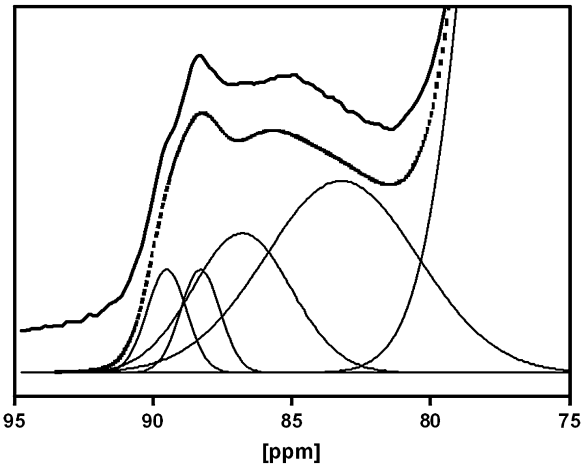

Fig. 10. Result of fitting exercise for C4 region of as-received lyocell fibre. Simulation with gaussian peaks of adjustable intensity, with constant shift and width (dashed line). Experimental spectrum *y*-shifted for clarity (bold line).

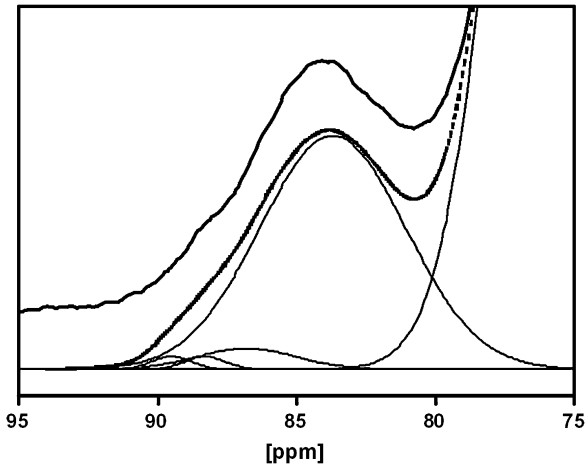

Fig. 12. Result of fitting exercise for C4 region of CM-lyocell fibre. Simulation (dashed line) with gaussian peaks of adjustable intensity with constant shift (fully-disordered peak at 83.5 ppm) and width. Experimental spectrum (bold line) *y*-shifted for clarity.

simulated envelope, reproducing the experimental effect seen with the fibre series in Fig. 3. In almost all cases respectable fits were achieved by adjustment of only individual peak intensities with no manipulation of line-width or shift positions, even for the microcrystalline samples. Although clearly a simplification, this approach does support the concept of polymer units in families of similar conformational states. The fitted intensities provide quantitative information about the distribution of order within the cellulosic material, with assignments based on controlled modifications to the physical polymer morphology.

From Table 1, the ratio of partially-ordered to crystalline-ordered intensity is higher for lyocell, cupro and polynosic fibres than the others in the series. This maybe related to the fibrillar character of these fibre morphologies and the narrow widths of the crystalline regions [28]. The fortisan high-performance fibre has a large amount of ordered polymer, as shown also in Fig. 3, and a lower partially-ordered to crystalline-ordered ratio, and may therefore have wider crystalline domains. The action of acid hydrolysis is shown to increase the proportion of crystalline order of both lyocell and viscose, which is at the expense of both the partially-ordered and fully-disordered environments. Recrystallisation may therefore affect sites with both hydroxymethyl and glycocidic bond disorders, which suggests that both these kinds of environments maybe found at crystal interfaces or defects, closely associated with crystalline domains. The recrystallisation process is also shown to reduce the partially-ordered to crystalline-ordered intensity ratio, which is consistent with an improvement in crystal width [31]. A similar but less exaggerated effect is achieved following wetting and re-drying of lyocell. The CM-lyocell sample has a small residual amount of crystalline order and also apparently a small degree of partial order. The respective intensity ratio also suggests the presence of very thin crystalline regions.

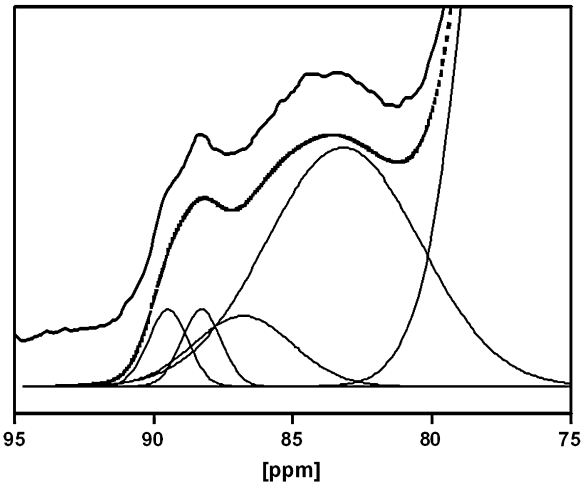

Fig. 11. Result of fitting exercise for C4 region of as-received viscose fibre. Simulation with gaussian peaks of adjustable intensity with constant shift and width (dashed line). Experimental spectrum *y*-shifted for clarity (bold line).

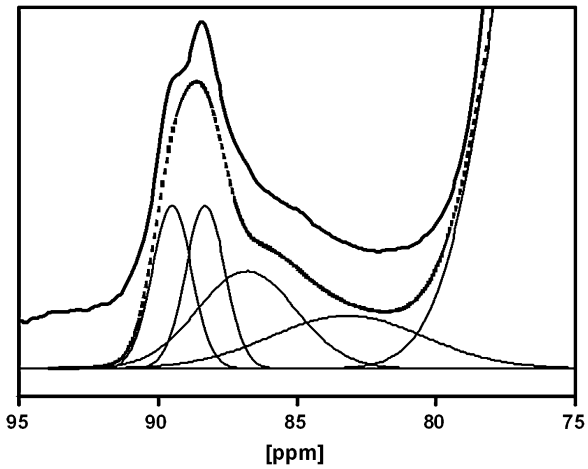

Fig. 13. Result of fitting exercise for C4 region of hydrolysed lyocell fibre. Simulation with gaussian peaks of adjustable intensities with constant shift and width (dashed line). Experimental spectrum *y*-shifted for clarity (bold line).

From chemical shifts alone it is not possible to say whether the C4 peak accounting for fully-disordered polymer is due to conformational environments associated with individual sites or an assembly within a separate morphological phase. It is likely that defects leading to glycocidic conformational freedom will have an impact on at least the next-neighbour chains, but this maybe a local influence rather than evidence of a true amorphous phase. However, the observation of small differences in H-$T_{1\rho}$ behaviour for the different C4 shifts is evidence of a domain structure extending over 2–3 nm, equivalent to maybe 5–6 polymer chain widths. The resolution of different H-$T_{1\rho}$ relaxation times may partly be explained by the presence of distinct crystallite entities within the supramolecular structure, accounting for the crystallographic splitting of the 89.5 and 88.3 ppm peaks. The partially-ordered C4 shift position shares a common H-$T_{1\rho}$ relaxation time with the crystalline-ordered shift, suggesting that this polymer is intimately associated with the crystallite entities, potentially as part of the same phase. However, the separately resolved H-$T_{1\rho}$ time measured at the fully-disordered C4 shift position suggests that such conformationally disordered sites are not incorporated within the crystalline phase or at the crystallite interfaces, otherwise a single averaged H-$T_{1\rho}$ value would be found across the C4 entire envelope.

True crystalline material must be definition be present as domains with repeating chain environments extending over several unit cell distances. In addition, in a well-oriented fibrillar cellulosic fibre, such as lyocell, the presence of a significant proportion of fully-disordered C4 intensity could be evidence of other domains exhibiting the so-called paracrystallinity, with atoms dislocated from crystal positions, but still associated with areas of true crystalline order [32]. A more heterogeneous model may therefore be appropriate to describe this and other regenerated cellulosic fibres, including a crystalline interfacial region that maybe extending over several chain widths, each layer tending towards greater conformational disorder and experiencing greater dynamic freedom. A diffuse, extended interfacial region would contain sites exhibiting both partial order and full conformational disorder, with accompanying crystalline-ordered domains possibly containing defect sites exhibiting partial order. Both partially and fully-disordered sites in the interface would experience recrystallisation during acid hydrolysis, leading to an apparent increase in crystal widths. The presence of both crystalline regions and diffuse interfacial regions would account for the partial separation of H-$T_{1\rho}$ relaxation times, with a greater thickness of the diffuse interfacial zone leading to a reduction in the measured H-$T_{1\rho}$ relaxation for both crystalline and non-crystalline C4 positions, as a result of spin-diffusion. The fitted data in Table 1 represent a simplification of the real sample heterogeneity but allow a quantitative measure of the material texture and the way in this depends on sample history or processing.

An analysis of the rotameric populations accounting for the full C4 envelope is beyond the scope of this paper. The influence of the conformation (χ angle) of the carbon or oxygen atoms' three bonds removed from the observed site (gamma) has been used empirically to rationalise chemical shift behaviour in saccharides and polymers [12,13]. A change from *trans* + *gauche* (tg) or *gauche* + *trans* (gt) to a *gauche* + *gauche* (gg) arrangement around the C5–C6 bond is believed to be responsible for a −3 ppm Carbon-13 shift [10]. Fixed tg and/or gt conformations are assumed to exist in the rigid cellulose II crystal form, which must become more variable due to defects and disorder [26,33]. An increase in gg arrangements seems reasonable, although it is difficult to imagine a uniform and constant bond angle for all such non-crystalline sites. A distribution of angles around a mean would account for the apparent broadening of non-crystalline peaks. In addition, the C2 gamma atom across the glycocidic bond may also influence the chemical shift of the C4 site, by virtue of rotation about the O1–C1 bond (ϕ angle). This is in a partially eclipsed position in the crystalline arrangement, as a result of the constraints of the ordered hydrogen-bonding network [4]. Disruption of hydrogen bonding would permit more staggered glycocidic conformations, possibly allowing the partial population of *gauche* C2–C1–O4–C4 arrangements. Without such conformational mobility it would not be possible for the cellulose chains to adopt more random paths, ultimately leading to the semi-flexible behaviour of the polymer in solution [34]. The increase in *gauche* arrangements would be expected to cause further negative shifts and broadening of the C4 resonance.

5. Conclusions

Studies of a range of regenerated cellulosic fibres have revealed systematic changes in chemical shifts of the Carbon-13 C4 spectral envelope, which can be related to the influence of chemical or physical modification of the polymer supramolecular structure. A full understanding of cellulosic fibre architecture will enable better prediction of the effects of commercial processing on fibre and textile performance. This work has developed existing concepts, where the C4 envelope is considered to be the sum of contributions from polymer in differing polymer conformational states, associated with differing degrees of order or disorder. Peaks in the C4 region have been previously assigned due to the fully ordered crystalline cellulose II allomorph, which are seen to a greater or lesser extent in all samples, representing polymer units with no conformational variability. The remaining intensity within the C4 envelope has been separated into two other broader peaks using a constrained curve fitting procedure. One broad peak is assigned to polymer units with intermediate order, where the hydroxymethyl group exhibits conformational variability. A further broader peak is assigned to fully-disordered polymer, where variability affects both the hydroxymethyl group and the glycocidic bond. The curve fitting exercise has been applied with success to a range of regenerated cellulosic materials, with the balance between ordered, partially-ordered and disordered intensities accounting for observed C4 features. In the majority of cases no adjustment of shifts or line-widths is necessary in the fitting exercise. The quantification of polymer units within different conformational groupings will provide additional insights concerning the size and

form of differing morphological regions in these cellulosic materials. A model is proposed where crystalline domains are bounded by a diffuse, non-crystalline interface, where polymer chains exhibit increasing disorder at greater distance from the crystal surface. The description of a heterogeneous structure is supported by data from proton rotating frame relaxation measurements. This work also supports the view that empirical gamma-*gauche* effect is likely to provide the best rationalization for the relationship between C4 shifts and conformational order. The broadness of the disordered C4 spectra features maybe accounted for by an increased statistical spread of rotameric positions of both the hydroxymethyl and glycocidic bonds.

Acknowledgements

The authors would like to thank Tom Rhöder of Lenzing AG for supply and preparation of fibre samples. Thanks also to Christian Schuster of Lenzing AG, for helpful discussions.

Financial support was provided by the Christian Doppler Society, the Austrian government, the provinces of Lower Austria, Upper Austria, and Carinthia as well as by Lenzing AG. We also express our gratitude to the Johannes Kepler University, Linz, the University of Natural Resources and Applied Life Sciences, Vienna, and the Lenzing AG for their kind contributions.

References

[1] Maunu SL. Prog Nucl Magn Reson 2002;40:151–74.
[2] Gill AM, Neto CP. Annu Rep NMR Spectrosc 1999;37:75–117.
[3] Earl WL, VanderHart DL. Macromolecules 1981;14:570–4.
[4] Kolpak FJ, Blackwell J. Macromolecules 1976;9:273–8.
[5] Sarko A, Stipanovic AJ. Macromolecules 1976;9:851–7.
[6] Kolpak FJ, Weih M, Blackwell J. Polymer 1978;19:123–31.
[7] Hofmann D, Fink D-P, Philipp B. Polymer 1989;30:237–41.
[8] Hirai A, Horii F, Kitamaru R. Cellul Chem Technol 1990;24:702–11.
[9] Newman RH, Hemmingson JA. Cellulose 1994;2:95–110.
[10] Newman RH, Davidson TC. Cellulose 2004;11:23–32.
[11] Horii F, Hirai A, Kitamaru R. ACS Symp Ser 1984;260:27–42.
[12] Tonelli AE. NMR spectroscopy and polymer microstructure: the conformational connection. NY: VCH Publishers; 1989. p. 46–53.
[13] Howarth O, Hobley P, Ibbett R. Magn Reson Chem 1996;34:755–60.
[14] Barfield M. J Am Chem Soc 1993;115:6916–28.
[15] Metz G, Wu X, Smith SO. J Magn Reson A 1994;110:219.
[16] Harris RK. Nuclear magnetic resonance spectroscopy – a physicochemical view. Harlow, UK: Longman Scientific and Technical; 1992 [chapter 6].
[17] Love GD, Snape CE, Jarvis MC. Biopolymers 1992;3:1187–92.
[18] Fife CA, Dudley RL, Stephenson PJ, Deslandes Y, Hamer GK, Marchessault RH. J Am Chem Soc 1983;105:2469–72.
[19] Maciel GE, Kolodziejski WL, Bertran MS, Bruce ED. Macromolecules 1982;15:686–7.
[20] Maier G, Zipper P, Stubičar M, Schurz J. Cellul Chem Technol 2005;39:167–77.
[21] Yokota H, Toshiya S, Horii F, Kitamaru R. J Appl Polym Sci 1990;41:783–91.
[22] Nevell TP. In: Nevell TP, Zeronian SH, editors. Cellulose chemistry and its applications. UK: Ellis Horwood Ltd.; 1983 [chapter 9].
[23] Sharples A. Trans Faraday Soc 1957;1003–13.
[24] Horii F, Hirari A, Kitamaru R, Sakurada I. Cellul Chem Technol 1985;19:513–23.
[25] Masson J-F, Manley RSJ. Macromolecules 1992;25:589–92.
[26] Langan P, Nishiyama Y, Chanzy H. Biomacromolecules 2001;2:410–6.
[27] Horii F, Hirai A, Kitamaru R. Polym Bull 1983;10:357–67.
[28] Crawshaw J, Cameron RE. Polymer 2000;41(12):4691–8.
[29] Bredereck K, Hermanutz F. Rev Prog Colour 2005;35:59–75.
[30] Hesse S, Jager C. Cellulose 2005;12:5–14.
[31] Larsson PT, Wickholm K, Iversen T. Carbohydr Res 1997;302:19–25.
[32] Hofmann D, Fink H-P, Philipp B. Polymer 1989;30:237–41.
[33] Heiner AP, Kuutti L, Teleman O. Carbohydr Res 1998;306:205–20.
[34] Rees DA, Smith PJC. J Chem Soc Perkin II 1975;836–40.